

## Supporting Information

# Performance Evolution of CsPbI<sub>2</sub>Br Perovskite Solar Cells under Space-Equivalent Stressors

Sahil Verma, Lethy Krishnan Jagadamma\*

*Energy Harvesting Research Group, School of Physics & Astronomy, SUPA,  
University of St Andrews, North Haugh, St Andrews, Fife KY16 9SS, United Kingdom  
Email: lkj2@st-andrews.ac.uk*

## Experimental Methods

### Materials

Cesium iodide (CsI) and hydrogen lead trihalide (HPbX<sub>3</sub>) were purchased from Xi'an Polymer Light Technology Corp. Cesium formate (HCOOCs) was obtained from Alfa Aesar. Anhydrous dimethyl sulfoxide (DMSO, ≥99.9%) was sourced from Sigma-Aldrich. A colloidal dispersion of tin(IV) oxide (SnO<sub>2</sub>), used as the electron transport layer (ETL), was also acquired from Alfa Aesar. The hole transport layer (HTL) components included Spiro-OMeTAD [2,2',7,7'-tetrakis(N,N-di(4-methoxyphenyl)amino)-9,9'-spirobifluorene, >99%], 4-tert-butylpyridine (tBP, 96%), lithium bis(trifluoromethanesulfonyl)imide (Li-TFSI, 99.95%), and FK209[tris(2-(1H-pyrazol-1-yl)-4-tert-butylpyridine)cobalt(III) tris(bis(trifluoromethane)sulfonimide)]. These were procured from Ossila, Sigma-Aldrich, and Greatcell Solar Materials.

### Device Fabrication

Commercially available, pre-patterned indium tin oxide (ITO)-coated glass and fused silica substrates were used as the transparent conducting electrodes. These substrates underwent sequential cleaning, involving immersion in an aqueous sodium dodecyl sulfate (SDS) solution, deionised water, acetone, and isopropyl alcohol, with each step accompanied by ultrasonication to remove surface contaminants. Following this, the substrates were dried under N<sub>2</sub> blower and treated with UV-ozone (Ossila) for 15 minutes to enhance surface wettability and remove residual organic species.

For the electron transport layer (ETL), a tin(IV) oxide (SnO<sub>2</sub>) colloidal dispersion was diluted with deionized water in a 1:6.5 volume ratio. Approximately 100 μL of the diluted SnO<sub>2</sub> solution was deposited onto the prepared substrates via spin coating at 3000 rpm for 30 seconds.

This was followed by thermal annealing at 150 °C for 30 minutes to ensure the formation of a uniform and compact SnO<sub>2</sub> layer serving as an effective electron-selective contact. The SnO<sub>2</sub> coated ITO substrates were again treated with UV-Ozone for 15 minutes before the perovskite layer deposition.

The CsPbI<sub>2</sub>Br perovskite active layer was deposited using the spin-coating method. The perovskite precursor composition consisted of 1 mmol cesium formate (HCOOCs), 2/3 mmol HPbI<sub>3</sub>, and 1/3 mmol HPbBr<sub>3</sub>. The composition was dissolved in 1 mL of anhydrous dimethyl sulfoxide (DMSO) and stirred overnight to yield a 1 M solution. The perovskite precursor handling and the solution preparation were done inside a N<sub>2</sub> filled glovebox. The perovskite films were fabricated under ambient air without any deliberate humidity control. However, the average relative humidity was in the range of 42-46%. Before spin-coating, the substrates were preheated on a hotplate at 60 °C for 10 minutes to promote uniform film formation. A volume of 90 μL of the perovskite solution was dispensed onto the SnO<sub>2</sub>-coated 60 °C preheated substrates and subjected to a two-step spin-coating process: 1000 rpm (1000 ramp) for 10 seconds followed by 4000 rpm (2000 ramp) for 30 seconds. The resulting films were thermally annealed in two stages: at 60 °C for 10 minutes to allow solvent evaporation, and then at 250 °C for 10 minutes to crystallise the perovskite phase.

To form the hole transport layer (HTL), Spiro-OMeTAD (72.3 mg) was dissolved in 1 mL of chlorobenzene. Additives were introduced to enhance its conductivity: 28.8 μL of 4-tert-butylpyridine (tBP), 17.5 μL of a Li-TFSI solution (prepared by dissolving 52 mg Li-TFSI in 100 μL acetonitrile), and 29 μL of an FK209 solution (30 mg in 100 μL acetonitrile). A volume of 55 μL of the resulting HTL solution was spin-coated onto the perovskite layer at 4000 rpm for 30 seconds. The samples were left in a desiccator at ambient temperature overnight to facilitate oxidation of Spiro-OMeTAD overnight at ambient temperature to facilitate Spiro-OMeTAD oxidation under ambient oxygen exposure. Finally, an 80 nm thick gold (Au) electrode was deposited via thermal evaporation under high vacuum conditions ( $\sim 3 \times 10^{-6}$  mbar). The effective device area was defined as 0.1 cm<sup>2</sup>.

## **Characterization of the Devices and Films**

After establishing the fabrication process, the performance of the fabricated perovskite solar cells was evaluated using a custom-built measurement system. Space environment testing was conducted within a Linkam Scientific vacuum stage, enabling precise modulation of temperature and pressure to simulate conditions representative of the near-space environment.

Measurements were performed at reduced pressures (down to  $10^{-3}$  mbar) and over a temperature range of  $+150^{\circ}\text{C}$  to  $-150^{\circ}\text{C}$ , with illumination under AM0 conditions at a ramp rate of  $30^{\circ}\text{C}/\text{min}$  to mimic extraterrestrial spectral profiles.

Current density–voltage ( $J$ – $V$ ) characteristics were recorded under two solar spectra. For AM0 testing, G2V Pico solar simulator [(Pico Solar Simulator KLMNO (350-1500nm)] delivering an irradiance of  $85.2\text{ mW cm}^{-2}$  was employed. The irradiance spectrum of this AM0-like illumination is given in Figure S1.

For terrestrial benchmarking, a Sciencetech Class AAA solar simulator equipped with a 150 W xenon arc lamp was used to provide AM1.5G illumination, calibrated to  $100\text{ mW cm}^{-2}$ . All  $J$ – $V$  measurements were conducted using an Ossila Source Measure Unit (SMU) interfaced with dedicated solar cell IV analysis software.

A metal shadow mask was applied during AM1.5G testing to define the device's active area at  $0.05\text{ cm}^2$ . For the AM0 measurements, the device's active area used is  $0.1\text{ cm}^2$ . Voltage scans were executed in both forward ( $-0.1\text{ V}$  to  $1.5\text{ V}$ ) and reverse ( $1.5\text{ V}$  to  $-0.1\text{ V}$ ) directions, using a step size of  $0.05\text{ V}$ , a scan rate of  $0.2\text{ V s}^{-1}$ , and a dwell time of  $0.2\text{ s}$  at each measurement point.

The optical absorption characteristics of the  $\text{CsPbI}_2\text{Br}$  thin films were assessed using a Jasco V-760 UV–vis spectrophotometer, spanning the spectral range of 300 to 900 nm. To probe charge carrier dynamics and recombination behaviour, light-intensity-dependent  $J$ – $V$  measurements were conducted, along with impedance spectroscopy and transient photocurrent (TPC) analyses. These were performed using the Paios all-in-one characterization platform (Fluxim AG, Switzerland). Structural analysis of the perovskite films was carried out using X-ray diffraction (XRD) on a Bruker D8 Discover diffractometer equipped with a 2D EIGER2R-500K detector. Measurements utilized  $\text{Cu K}\alpha_1$  radiation ( $\lambda = 1.5406\text{ \AA}$ ), with scans performed across a  $2\theta$  range of  $5^{\circ}$  to  $80^{\circ}$ , at a step size of  $0.02^{\circ}$  and a dwell time of 1 s per point. Surface morphology and grain structure were examined using field emission scanning electron microscopy (FESEM), conducted on a HITACHI S-4800 system. The acceleration voltage was 1.5–2 kV and the working distance was 6–10 mm.

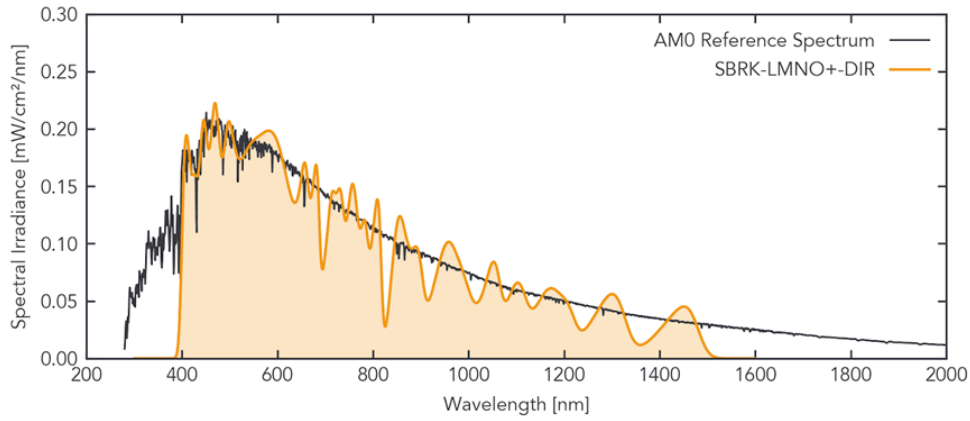


**Figure S1:** The irradiance spectrum of the AM0-like illumination used in this study compared with the AM0 Reference Spectrum.

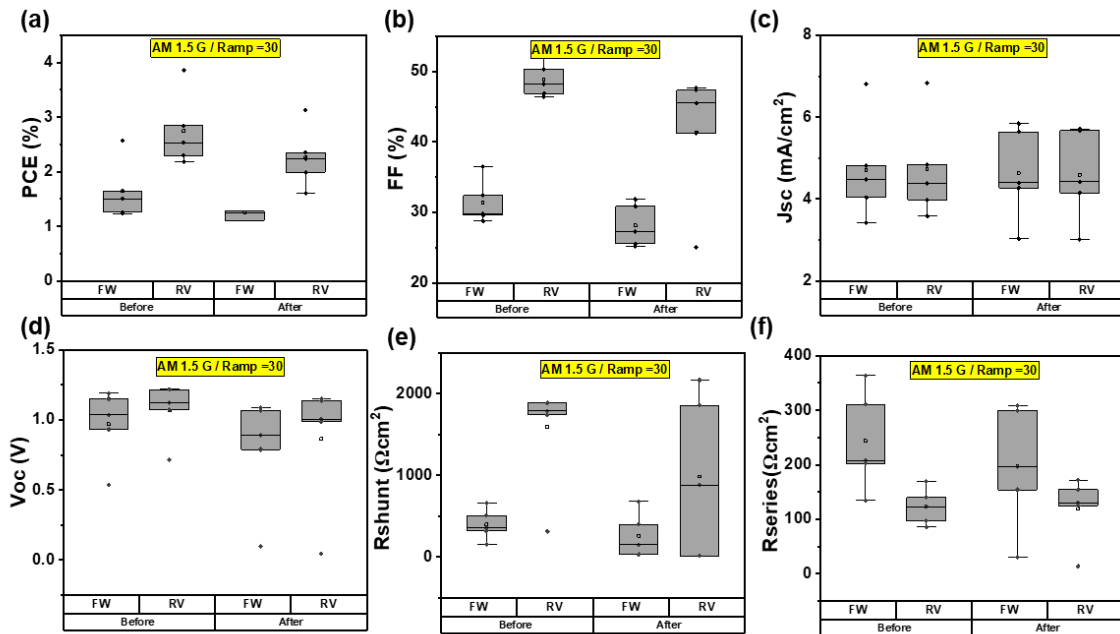


**Figure S2:** Box plots of photovoltaic performance parameters of CsPbI<sub>2</sub>Br devices fabricated on glass substrate, measured under AM 1.5 G illumination, before and after thermal treatment under AM0 with a ramp rate of 30°C/min. Parameters shown include: (a) *PCE*, (b) *FF*, (c) *J<sub>SC</sub>*, (d) *V<sub>OC</sub>*, (e) *R<sub>shunt</sub>*, and (f) *R<sub>series</sub>*. In these statistical box plots, the width of the box represents the range where 25% to 75% of the data points lie, the middle horizontal line indicates the median (typical) value, and the whiskers show the boundary of typical data. Some outlier data points are also shown in these plots.

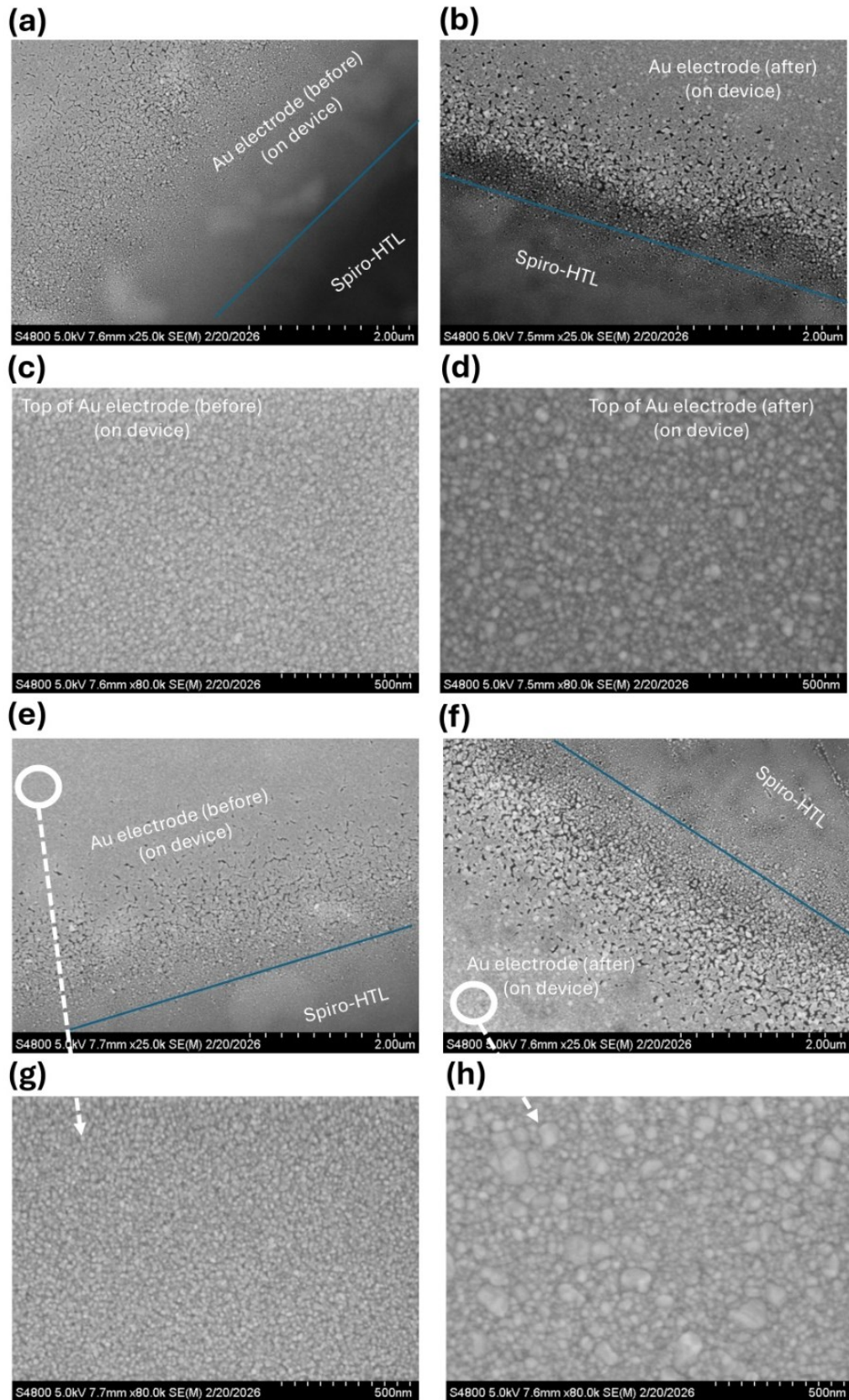


**Figure S3:** FESEM images of the CsPbI<sub>2</sub>Br perovskite solar cell gold contact layer on glass/ITO (a-d) and (e-h) Fused silica/ITO substrates.

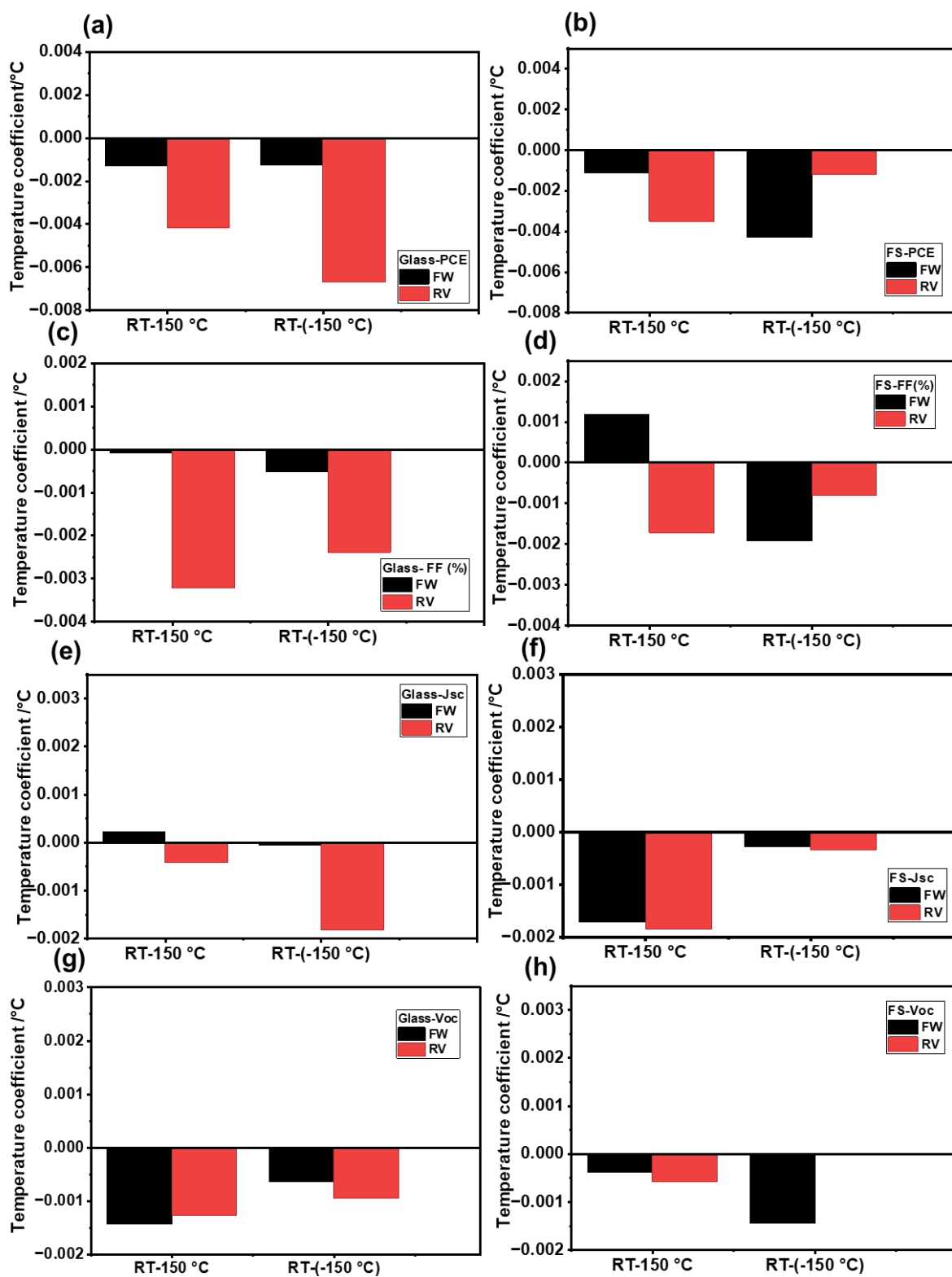


**Figure S4:** Temperature coefficient of photovoltaic parameters ( $PCE$ ,  $FF$ ,  $J_{sc}$ ,  $V_{oc}$ ) of  $CsPbI_2Br$  perovskite solar cells fabricated on (a,c,e,g) glass and (b,d,f,h) fused silica substrates.

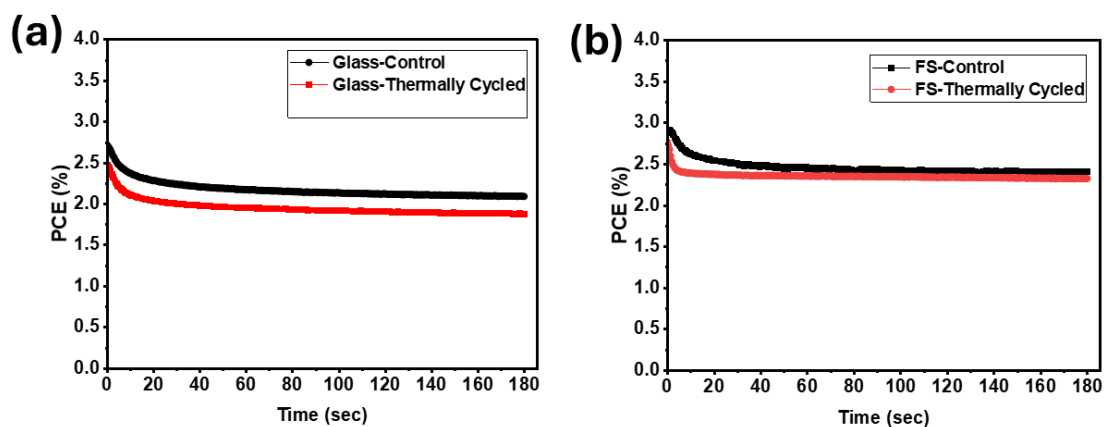


**Figure S5:** Steady state *PCE* under AM0-like illumination of (a) glass and (b) fused silica substrate-based devices before and after thermal cycling.

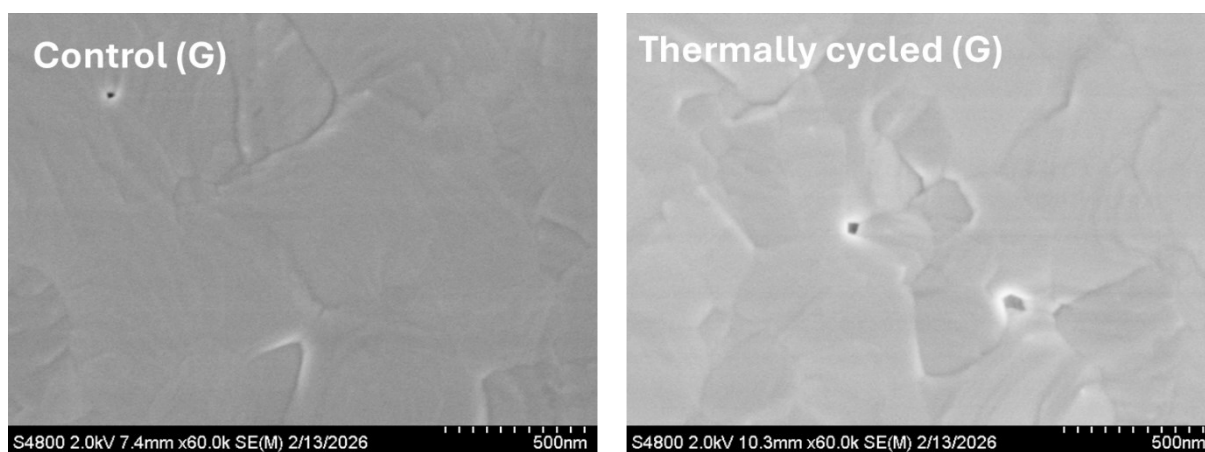


**Figure S6:** High-resolution FESEM images of the Glass/ITO/CsPbI<sub>2</sub>Br films before and after thermal cycling.

**Table S1:** Derived parameters from impedance spectroscopy for glass-based devices under test

<b>Substrate type</b>	<b>Type of devices</b>	<b>Series resistance (Rs)</b>	<b>Electronic resistance (M<math>\Omega</math>)</b>	<b>Ionic resistance (k<math>\Omega</math>)</b>	<b>Geometric capacitance (nF)</b>	<b>Ionic capacitance (nF)</b>
<b>Glass</b>	Control	37.5	7.39	5.0	24.7	15
	Thermally Cycled	40.4	4.96	2.0	29.2	8
	Recovery	49.3	11.0	2.0	22	8

**Table S2:** Derived parameters from impedance spectroscopy for fused silica based devices under test

<b>Substrate type</b>	<b>Type of devices</b>	<b>Series resistance (Rs)</b>	<b>Electronic resistance (M<math>\Omega</math>)</b>	<b>Ionic resistance (k<math>\Omega</math>)</b>	<b>Geometric capacitance (nF)</b>	<b>Ionic capacitance (nF)</b>
<b>Fused silica</b>	Control	176	24.6	3.0	20.7	1
	Thermally Cycled	40	8.5	1.0	30.3	10
	Recovery	60.5	20	1.0	26.8	50